

Analysis of Diffusion Induced Deformation Considering Electro-Migration in Lithium-ion Batteries

Xiaoming Liu¹, Hai Hu¹, Yaohong Suo^{1,2,*}, Pengfei Yu^{1,3,*}

¹ School of Mechanical Engineering and Automation, Fuzhou University, Fuzhou, 350108, China

² Key Laboratory of fluid Power and Intelligent Electro-Hydraulic Control (Fuzhou University), Fujian Province University, Fuzhou 350116, China

³ State key lab for strength and vibration of mechanical structures, School of Aerospace, Xi'an Jiaotong University, Xi'an 710049, China

*E-mail: yaohongsuo@126.com, yupengfei0422@fzu.edu.cn

Received: 5 March 2020 / Accepted: 13 April 2020 / Published: 10 June 2020

Electro-migration, diffusion-induced stress and their interaction have a significant impact on the electrode materials' performance and reliability. However, electro-migration is neglected in most existed models. In this work, a coupled electro-chemo-mechanical model with electro-migration is developed by using Gauss law, mass balance and equilibrium equation. The diffusion flux is separated into two parts: one is the gradient of concentration, and the other is the coupling terms including the concentration-hydrostatic pressure gradient term and the concentration-electric potential gradient term. Then some numerical simulations in a hollow spherical electrode of LiMn₂O₄ are carried out under potentiostatic and galvanostatic operations to capture how the electro-migration impacts on the lithium-ion concentration, radial stress and hoop stress. The numerical results reveal that the electro-migration plays a significant role in the diffusion (lithium-ion concentration) and mechanical deformation in the hollow spherical electrode for larger diffusion time; when the electrical potential at the inner surface is smaller than that at the outer surface, the charging efficiency will be improved and the stresses in the electrode will be descended.

Keywords: Lithium-ion battery; Electro-chemo-mechanical coupling; Electro-migration; Diffusion-induced stress

1. INTRODUCTION

More and more attentions of lithium-ion batteries (LIB) are wildly paid due to its higher energy storage density and longer life [1, 2]. During the process of lithiation or de-lithiation in LIB, many electrode materials suffer from interactions of multi-physical field or multi-physical process. For example, intercalation or deintercalation (diffusion) of lithium-ion in the electrode can cause the

volume change of the electrode [3-5], result in inhomogeneous expansion or contraction [6]. As a result, mechanical stress generates which is called as diffusion-induced stress (DIS) [7] by an analogy to thermal stress. Larger stress will make the electrode crack [8], failure and even damage, which leads to battery degradation, the effective capacity decrease and shorter service life. Therefore, it is vital to investigate lithium-ion diffusion and stress distribution to improve the effective capacity and service life.

Diffusion induced stress plays a significant role in the capacity fade and cycle/calendar life. The first model [7] of diffusion-induced stress can be dated back to the 1960s by Prussin, who achieved the stresses developed in Si wafers by using the method similar to the thermal stress. Following this, a series of researches are published to investigate this problem. For instance, Lee et al. [9] presented an analytical solution of diffusion-induced-stress in a hollow cylinder with constant surface stresses. Zhang et al. [10] investigated the diffusion-induced stress in the different spherical and ellipsoidal electrode, and pointed out that smaller size electrode is helpful to decrease the stress. Ji and Guo [11] considered diffusion, diffusion-induced stress, Butler-Volmer reaction kinetics and size polydispersity of electrode particles and developed an analytical model of porous electrode by adopting the Gibbs free energy. Zhang et al. [12] proposed a modified Cahn-Hilliard type phase-field model and derived an analytical expression for the local flux induced by the local deformation velocity. Suo and Yang [13] analyzed the transient diffuse-induced-deformation in the viscoelastic polymer polypyrrole (PPY) electrode. Li et al. [14] considered the interaction among solute atoms, local deformation velocity and viscoplasticity in a large-deformed electrode and described diffusion-induced deformation from the framework of the generation of defects due to the migration of solute atoms. Suo and Yang [15] developed a one-dimensional reaction-diffusion-stress fully coupled model in lithium-ion battery. Cheng and Verbrugge [16] presented analytic expressions for the evolution of stress and strain energy within a spherically shaped electrode element under either galvanostatic (constant current) or potentiostatic (constant potential) operation. Zhang et al. [17] simulated the intercalation-induced stress and heat generation inside Li-ion battery cathode (LiMn_2O_4) particles under potentiodynamic control. However, the impact of the electro-migration on the diffusion of the lithium-ions and deformation of the electrode is not taken into account in these above researches.

The electrical potential in the electrode particle is variable due to the current flow during the charge or discharge in the lithium-ion battery and its gradient will drive the lithium-ion diffusion [18]. Thus, the effect of the electrical field on the diffusion should be involved in the diffusion equation. At present, more attentions of electro-chemo-mechanics are focused on the theories and experimental observations. For example, Golmon et al. [19] simulated the insertion of lithium into spherical silicon particles by using a fully-coupled diffusion-elasticity model with Butler-Volmer surface kinetics. Wan and Ciucci [20] gave some theoretical investigations on electro-chemo-mechanical coupling in the lithium ion batteries and solid oxide fuel cells. A finite strain theory for electro-chemo-mechanics of LIB electrodes along with a monolithic and unconditionally stable finite element algorithm for the solution of the resulting equation systems was proposed by Dal and Miehe [21]. Mohanty et al. [22] illustrated the role of elastic driving forces on the concentration, stress distributions and the current-voltage relations under potentiostatic and potentiodynamic operation. Mei et al. [23] developed a three-dimensional electro-chemo-mechanical model at the particle level for a $\text{LiMn}_2\text{O}_4/\text{Graphite}$ battery.

However, electro-chemo part in the aforementioned electro-chemo-mechanical coupling models is usually regarded to be electrochemical reaction described by the Butler-Volmer kinetic model, and the electrical potential effect on the diffusion and mechanical stress is lacking. Based on the lacking, the present paper will consider the influence of the electro-migration on the diffusion and stresses, take the hollow spherical electrode particle to be an object and develop an electro-chemo-mechanical coupling model to discuss the effect of electrical field on the charge efficiency. This coupled model in this work will provide the structure design guidance for high performance and long cycle life.

2. MATHEMATICAL MODEL

Consider the deformation of a hollow spherical electrode with the inner radius r_0 and outer radius r_1 , and its schematics is shown in Fig. 1.

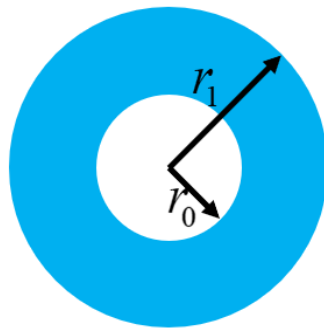


Figure 1. Sketch of hollow spherical electrode

For simplicity, the following assumptions are made: (1) The deformation of the electrode is small, and the theory of linear elasticity can be used in the description of the deformation of the electrode; (2) The whole charge/discharge process is isothermal; (3) The electrode is isotropic, and the materials properties are independent of concentration and mechanical deformation; (4) Diffusion and electrical potential only happen in the radial direction.

2.1 Electrical field equations

The relationship [24] of the electrical displacement D_r and electric field intensity E_r is as follows

$$D_r = \epsilon_0 E_r \quad (1)$$

where ϵ_0 is the dielectric constant and the subscript r denotes the radial direction.

The electric field intensity E_r can be expressed by the electric potential φ as

$$E_r = -\frac{d\varphi}{dr} \quad (2)$$

During the charge or discharge, lithium ions and electron insert or migrate the electrode

simultaneously and the spherical electrode will satisfy the electro-neutrality condition. Based on the Gauss theory, the electrical displacement equation is

$$\frac{dD_r}{dr} + \frac{2D_r}{r} = 0 \quad (3)$$

Substituting Eqs. (1) and (2) into (3), the Laplace equation can be obtained

$$\frac{d^2\varphi}{dr^2} + \frac{2}{r} \frac{d\varphi}{dr} = 0 \quad (4)$$

Suppose that the electrical potentials at the inner and outer surface are φ_0 and φ_1 , respectively.

That is,

$$\varphi|_{r=r_0} = \varphi_0, \quad \varphi|_{r=r_1} = \varphi_1 \quad (5)$$

An analytical solution of φ is given by solving Eq. (4) associated with Eq. (5)

$$\varphi = \varphi_0 + \frac{\varphi_0 - \varphi_1}{r_0 - r_1} r_1 \left(1 - \frac{r_0}{r}\right) \quad (6)$$

2.2 Mechanical equations

Similar to the thermal strain, the stress-strain constitutive equation [10] with diffusion-induced deformation becomes

$$\varepsilon_r = \frac{1}{E} (\sigma_r - 2\nu\sigma_\theta) + \frac{\Omega}{3} c \quad (7)$$

$$\varepsilon_\theta = \frac{1}{E} [\sigma_\theta - \nu(\sigma_r + \sigma_\theta)] + \frac{\Omega}{3} c \quad (8)$$

where ε_r and ε_θ are the radial and hoop strain, respectively. σ_r and σ_θ are the corresponding radial stress and hoop stress. E , ν , Ω and c are the Young's modulus, Poisson's ratio, the partial molar volume, and lithium-ion concentration, respectively.

According to the theory of linear elasticity, the radial strain ε_r and the hoop strain ε_θ can be calculated by the radial displacement u in the following

$$\varepsilon_r = \frac{\partial u}{\partial r}, \quad \varepsilon_\theta = \frac{u}{r} \quad (9)$$

The equilibrium equation without body force in the spherical electrode can be written as

$$\frac{\partial \sigma_r}{\partial r} + \frac{2}{r} (\sigma_r - \sigma_\theta) = 0 \quad (10)$$

Substituting Eqs. (7-9) into (10), one can obtain the equilibrium equation

$$\frac{\partial^2 u}{\partial r^2} + \frac{2}{r} \frac{\partial u}{\partial r} + \frac{2u}{r^2} = \left(\frac{1+\nu}{1-\nu}\right) \frac{\Omega}{3} \frac{\partial c}{\partial r} \quad (11)$$

It is noted that the equilibrium equation is associated with the displacement and concentration.

Suppose that the initial displace is zero and there are no constraints at the inner and outer surface. Thus, the initial condition and mechanical boundary conditions are given by

$$u|_{t=0} = 0 \quad (12)$$

$$\sigma_r|_{r=r_0} = \sigma_r|_{r=r_1} = 0$$

2.3 Diffusion equations

The driving for the lithium-ions diffusion/migration in the electrode is the gradient of the electro-chemical potential. The electro-chemical potential [24, 25] is sensitive to the concentration of lithium-ion (diffusion), the hydrostatic stress (mechanics) and electrical potential (migration). That is,

$$\mu = \mu_0 + R_g \theta \ln c - \Omega \sigma_h + Fz\varphi \quad (13)$$

where μ is the electro-chemical potential (J/mol), μ_0 is the chemical potential at the reference state with stress-free state and no electrical potential. R_g is the gas constant, θ is the absolute temperature, $\sigma_h = (\sigma_r + 2\sigma_\theta)/3$ is the hydrostatic pressure, F (=96485.3 C mol⁻¹) is the Faraday constant, and z is the charge number of lithium ions.

The diffusion flux J is governed by the gradient of the electro-chemical potential

$$J = -cM \frac{\partial \mu}{\partial r} \quad (14)$$

where $M = D/R_g \theta$ is the mobility of lithium ions in the electrode.

The diffusion equation of lithium-ion in the electrode is

$$\frac{\partial c}{\partial t} + \frac{1}{r^2} \frac{\partial}{\partial r} (r^2 J) = 0 \quad (15)$$

Substituting Eq. (13) and (14) into (15) yields

$$\frac{\partial c}{\partial t} = \frac{1}{r^2} \frac{\partial}{\partial r} \left[r^2 D \left(\frac{\partial c}{\partial r} - \frac{\Omega c}{R_g \theta} \frac{\partial \sigma_h}{\partial r} + \frac{Fzc}{R_g \theta} \frac{\partial \varphi}{\partial r} \right) \right] \quad (16)$$

Combining Eq. (6) into (16), the diffusion equation affected by the stress and electrical field is obtained

$$\frac{\partial c}{\partial t} = \frac{1}{r^2} \frac{\partial}{\partial r} \left\{ r^2 D \left[\frac{\partial c}{\partial r} - \frac{\Omega c}{R_g \theta} \frac{\partial \sigma_h}{\partial r} + \frac{Fzc(\varphi_0 - \varphi_1)r_0 r_1}{R_g \theta(r_0 - r_1)} \frac{1}{r^2} \right] \right\} \quad (17)$$

Suppose the initial concentration of lithium ions in the electrode is zero and lithium-ions diffuse from the outer surface to the inner. Two cases (potentiostatic and galvanostatic operation) are discussed for the lithiation. Thus, the corresponding initial and boundary conditions are, respectively, written as

$$c|_{t=0} = 0 \quad (18)$$

Case I Potentiostatic operation

$$J|_{r=r_0} = 0, \quad c|_{r=r_1} = c_0 \quad (19)$$

Case II Galvanostatic operation:

$$J|_{r=r_0} = 0, \quad J|_{r=r_1} = \frac{I_n}{F} \quad (20)$$

where I_n is the current density.

It is easy to find from the above analysis that Eqs. (6), (11) and (17) are made up of the coupling electro-chemo-mechanical model equations. Noticing that the effect of the electrical field on the diffusion and stress is taken into account in this work, but the influence of the diffusion and deformation on the electrical potential or electrical displacement is lacking for the sake of simplify. Additionally, if the effect of the stress and electrical potential on diffusion is neglected, Eq. (17) will

reduce pure diffusion.

3. NUMERICAL RESULTS AND DISCUSSION

In order to investigate the evolutions of the concentration and stress affected by the electrical field in the hollow-spherical electrode, the electrode is supposed to be LiMn_2O_4 . The material parameters used in the numerical simulation is listed in Table 1.

Table 1. the value of the parameters in the numerical calculation

Parameter	Value	Units
Young's modulus E	10.0 [26]	GPa
Poisson ratio ν	0.3[26]	/
Partial molar volume Ω	3.497×10^{-6} [26]	m^3/mol
Diffusion coefficient D	7.08×10^{-15} [26]	m^2/s
Boundary concentration c_0	2.29×10^4 [26]	mol/m^3
Current density I_n	5.2	A/m^2
Temperature θ	293.15	K
Gas constant R_g	8.314	J/(mol·K)
Lithium-ion charge z	1.0	/
Inner radius r_0	1.0×10^{-6}	m
Outer radius r_1	10.0×10^{-6}	m

For the sake of discussion, let $\Delta\varphi = \varphi_1 - \varphi_0$, which expresses the electrical potential difference applied at the inner and outer surfaces of the hollow sphere. Obviously, when $\Delta\varphi = 0$, one can derive that there is no effect of the electrical field on the diffusion according to Eq. (17), and in fact its results are Zhang et al.'s results [10]. When $\Delta\varphi > 0$ (the electrical potential at outer surface is larger than that at inner surface), it leads to the gradient of the electrical potential larger than zero, and vice versa for $\Delta\varphi < 0$. Fig. 2 plots the electrical potential distributions with respect to the radius r/r_1 for different $\Delta\varphi$. It can be observed that the magnitude of the electrical potential gradually increases with the increase of r/r_1 except for $\Delta\varphi = 0$. However, the electrical potential is constant in the whole electrode for $\Delta\varphi = 0$, which matches with the analysis of Eq. (6). At a fixed spatial position, the electrical potential will be larger for the larger magnitude of $\Delta\varphi$. Additionally, the magnitude of the electrical potential rises up quickly at smaller r/r_1 , which means the larger electrical potential gradient. Whereas the magnitude of the electrical potential changes slowly and there is a smaller electrical potential gradient at larger r/r_1 .

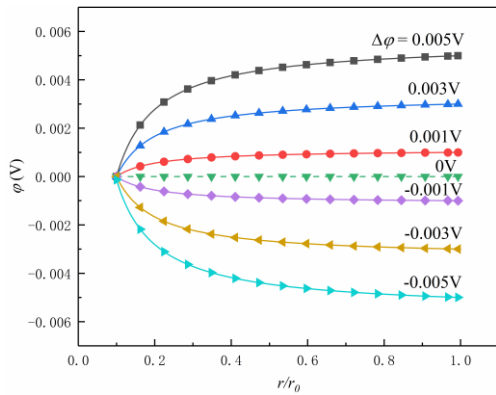


Figure 2. Distributions of the electric potential with respect to the radius r / r_1 for different $\Delta\varphi$

Case I Potentiostatic operation:

Figure 3 describes the distributions of lithium-ion concentration and the stresses (radial and hoop stress) for different electrical potential under the potentiostatic operation. The concentration variation with the radius at different charge time T ($= Dt / r_i^2$) for $\Delta\varphi > 0$ is shown in Fig. 3(a). With the increase of the lithiation time, more and more lithium-ions diffuse into the electrode which leads to the increase of the lithium-ions concentration at a fixed spatial position in the electrode. When the diffusion time is longer, the concentration decreases first and then increases with the increase of the distance away from the outer surface. This phenomenon is due to that when the diffusion distance (away from the outer surface) is smaller, the concentration gradient is larger and it is the main driving force. Thus, the concentration firstly gradually reduces. However, when the diffusion distance is larger (i.e., r / r_1 is smaller), there exists larger and positive gradient of the electrical potential as shown in Fig. 2 for $\Delta\varphi > 0$, and the gradient of the electrical potential becomes the main driving force which causes more lithium ions to diffuse in the electrode and results in larger concentration. Therefore, the concentration declines first and then rises up as r / r_1 decreases gradually.

Figure 3(b) exhibits the spatial distribution of lithium-ion concentration for different $\Delta\varphi$ at $T = 0.1062$. Seen from Fig. 3(b), $\Delta\varphi$ has negligible effect on the concentration for larger r / r_1 whereas it plays a significant role on the concentration for smaller r / r_1 , and larger $\Delta\varphi$ causes larger concentration. When $\Delta\varphi$ is larger than zero, electrical field will improve to diffuse from the outside to inside. However, the diffusion of lithium-ion will be retarded when the gradient of the electrical potential is less than zero (i.e., $\Delta\varphi < 0$). This variation trend of the concentration is similar to that in reference [27]. In addition, it is reasonable from Fig. (3b) that the curve with $\Delta\varphi = 0$ (no effect of the electrical field on the diffusion) lies in the middle of curves with $\Delta\varphi > 0$ and $\Delta\varphi < 0$.

Fig. 3(c) and 3(d) show the stress distributions in the radial and hoop directions at $T = 0.1062$ for different $\Delta\varphi$, respectively. It can be observed that the radial stress in the electrode is tensile, whereas the hoop stress is tensile near the inner surface and compressive near the outer surface, which has been proved by reference [28]. The radial stresses satisfy the mechanical boundary condition at the inner and outer surfaces of spherical electrode, and the hoop stress at $r / r_1 = 0.1$ (the inner surface) reaches the peak, which is the main reason of the electrode damage [29]. From 3(c) and 3(d), the radial and the hoop stresses are both smaller for $\Delta\varphi > 0$. However, they will become larger for $\Delta\varphi < 0$. Thus,

one can obtain from Figs. 3(a) ~ (d) that (1) the electro-migration has a vital effect on the diffusion and the stress distributions in the electrode; (2) the electro-migration with $\Delta\varphi > 0$ can improve the lithium-ion diffusion and decrease the stresses in the hollow spherical electrode.

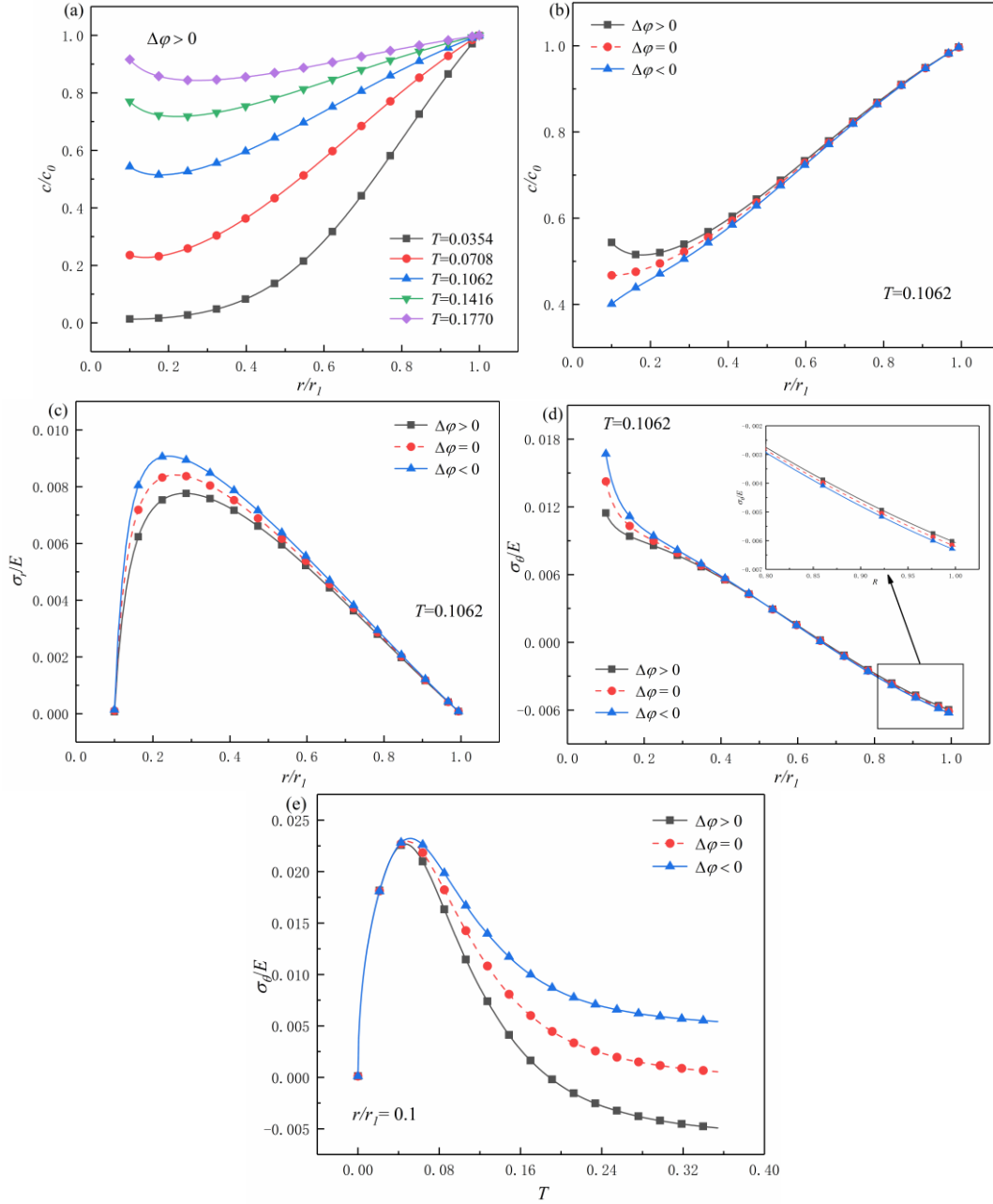


Figure 3. Case I: (a) Spatial distributions of concentration along radius for different T at $\Delta\varphi > 0$; (b) Concentration distribution along radius for different $\Delta\varphi$ at $T = 0.1062$; (c) Radial stress and (d) hoop stress along radius for different $\Delta\varphi$ at $T = 0.1062$; (e) Temporal distribution of hoop stress for different $\Delta\varphi$ at the location of $r/r_i = 0.1$.

Figure 3(e) depicts the temporal distribution of the hoop stress at the location of $r/r_i = 0.1$ for different $\Delta\varphi$. It is found that the hoop stress increases first, reaches the maximum and then decreases with the increase of the time whatever $\Delta\varphi$ is, which has been proved by [15, 30]. When the diffusion

time is shorter, $\Delta\varphi$ has negligible effect on the hoop stress. However, the influence of $\Delta\varphi$ is obvious for longer diffusion time. What's more, larger $\Delta\varphi$ effectively reduces the hoop stress. These signify that the influence of the electrical field on the diffusion and stress should not be omitted.

Case II Galvanostatic operation:

Figure 4 shows the distributions of lithium-ion concentration, radial and hoop stress for different electrical potential under the galvanostatic operation. The concentration distribution with r/r_i at different charge time for $\Delta\varphi > 0$ is exhibited in Fig. 4(a). The concentration of lithium-ions at a fixed spatial position gradually increases as the lithiation time increases. For larger time, the concentration decreases first and then increases with the decrease of r/r_i . When the diffusion time is shorter, the concentration gradually decreases with the increase of the distance away from the outer surface. The concentration variation trend under galvanostatic operation is similar to that under potentiostatic operation.

Figure 4(b) plotted the spatial distribution of lithium-ion concentration for different $\Delta\varphi$ at $T = 0.1416$ under galvanostatic operation. From Fig. 4(b), $\Delta\varphi$ has almost no influence upon the concentration near the outer surface, while it has a significant effect on the concentration near the inner surface. Moreover, larger $\Delta\varphi$ is, larger the concentration is. In addition, compared with the curve of $\Delta\varphi = 0$, the electrical field with $\Delta\varphi > 0$ will be helpful to diffuse from the outer to inner, and diffusion is retarded for $\Delta\varphi < 0$.

The distributions of the radial and hoop stress at $T = 0.1416$ for different $\Delta\varphi$ are shown in Fig. 4(c) and 4(d), respectively. The radial stress at the inner and outer surface is zero which coincides with the boundary condition (Eq. (12)) while it is tensile in the hollow spherical electrode in Fig. 4(c). At a fixed position, smaller $\Delta\varphi$ is, larger the radial stress is. The radial stress with $\Delta\varphi > 0$ is the smallest among these with $\Delta\varphi > 0$, $\Delta\varphi = 0$ and $\Delta\varphi < 0$. Seen from Fig. 4(d), the hoop stress is from tensile to compressive with the increase of r/r_i , and electro-migration has almost no influence on the hoop stress.

Similar to Fig. 3(e), the temporal distribution of the hoop stress at $r/r_i = 0.1$ for different $\Delta\varphi$ under galvanostatic operation is shown in Fig. 4(e). It is easily observed that the hoop stress first rises and then decreases with the increase of time no matter what $\Delta\varphi$ is. For shorter time, $\Delta\varphi$ has little effect on the hoop stress. However, the influence is obvious for longer time. Additionally, larger $\Delta\varphi$ is, smaller the hoop stress is. These results are also similar to those under galvanostatic operation.

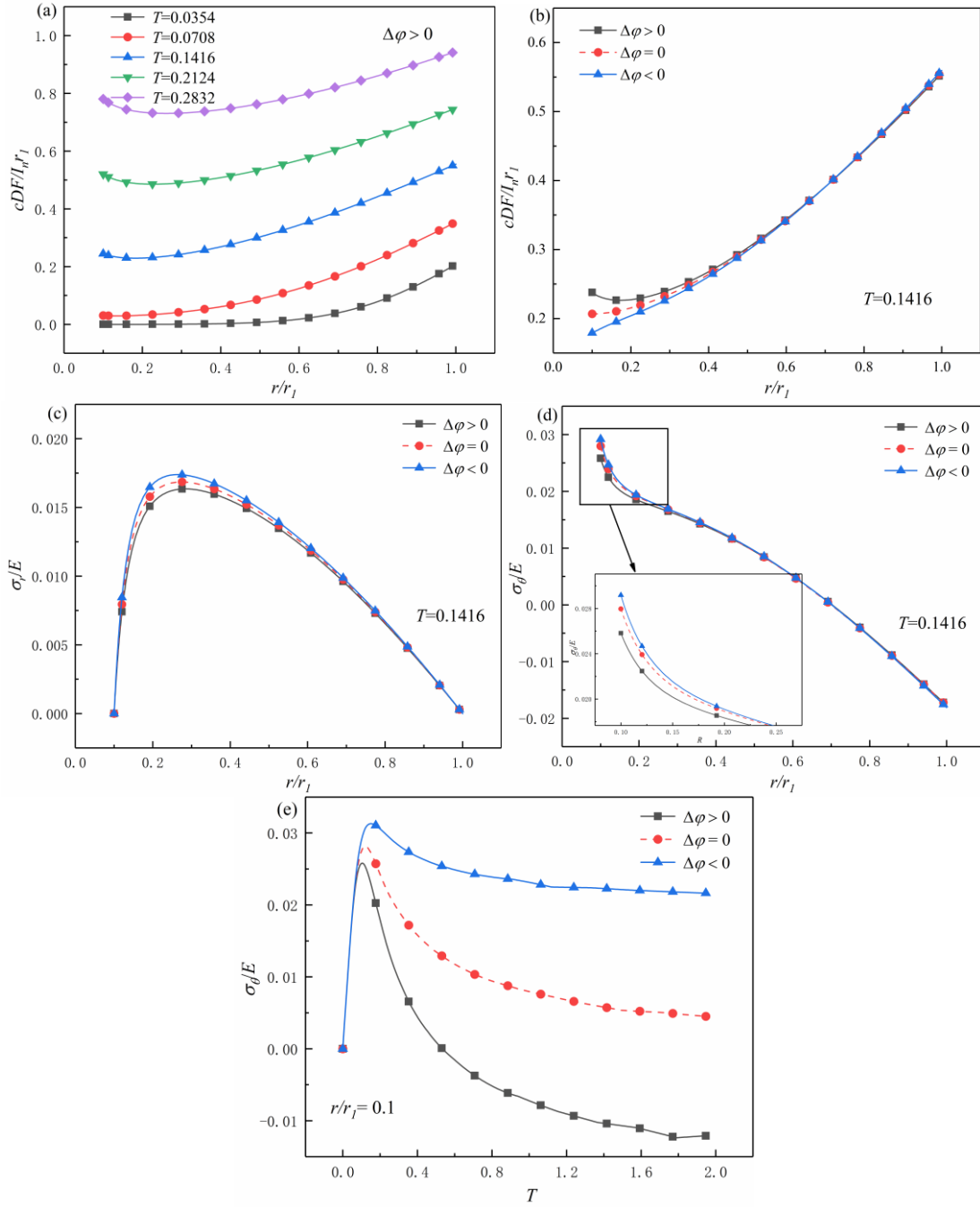


Figure 4. Case II: (a) Spatial distributions of concentration for different T at $\Delta\varphi > 0$; Spatial distributions of concentration (b), radial stress (c) and hoop stress (d) for different $\Delta\varphi$ at $T = 0.1416$; (d) temporal distribution of hoop stress for different $\Delta\varphi$ at $r/r_l = 0.1$.

4. CONCLUSION

In this work, the hollow spherical electrode is taken as an object. Taking into account the electro-migration effect on the diffusion and stresses, a coupled electro-chemo-mechanical model is developed on the basis of Gauss law, diffusion and mechanical equilibrium equation. Then taking LiMn_2O_4 as an example, the distributions of concentration, radial stress and hoop stress are calculated

under potentiostatic and galvanostatic operation, and how the electro-migration influences on the diffusion and stresses is also discussed. Numerical results indicate that 1) The electrical field affects not only lithium-ion diffusion but also the mechanical stresses in the electrode; 2) The electro-migration with $\Delta\varphi > 0$ is helpful to improve the lithium-ion diffusion and to decrease the radial and hoop stress. The proposed model can be used to analyze the batteries degradation behaviors and provide design guidance for improving charge efficiency.

ACKNOWLEDGEMENTS

The supports from NSFC (Grants No. 11902076), Natural Science Foundation of Fujian Provincial (No. 2018J01663, 2019J01634), Joint Fund for Tianjin and Fuzhou University (No. TF2020-2), Scientific Research Program Funded by Fujian Provincial Education Commission (No. JT180026) and 2018 Open Projects of Key Laboratory for Strength and Vibration of Mechanical Structures (No. SV2018-KF-25).

References

1. R. Rohan, Y.B. Sun, W.W. Cai, Y.F. Zhang, K. Pareek, G.D. Xu and H.S. Chen, *Solid State Ionics*, 268 (2014) 294.
2. L. Anand, *J. Mech. Phys. Solids*, 60 (2012) 1983.
3. R. Deshpande, Y. Qi and Y.T. Cheng, *J. Electrochem. Soc.*, 157 (2010) A967.
4. X. Gao, D.N. Fang and J.M. Qu, *Proc.: Math., Phys. Eng. Sci.*, 471 (2015) 20150366.
5. Y. Li, W.Y. Mao and K. Zhang, *J. Phys. D: Appl. Phys.*, 52 (2019) 435502.
6. H. Sitinamaluwa, J. Nerkar, M.C. Wang, S.Q. Zhang and C. Yan, *RSC Adv.*, 7 (2017) 13487.
7. S. Prussin, *J. Appl. Phys.*, 32 (1961) 1876.
8. H. Liu, M. Wolf and K. Karki, *Nano Lett.*, 17 (2017) 3452.
9. S. Lee, J.R. Chen and W.L. Wang, *Mater. Chem. Phys.*, 64 (2000) 123.
10. X.C. Zhang, W. Shyy and A.M. Sastry, *J. Electrochem. Soc.*, 154 (2007) A910.
11. L. Ji, Z.S. Guo, *Acta Mech. Sin.*, 34 (2018) 187.
12. K. Zhang, Y. Li and F. Wang, *J. Phys. D: Appl. Phys.*, 52 (2019) 145501.
13. Y.H. Suo, F.Q. Yang, *AIP Adv.*, 9 (2019) 065111.
14. Y. Li, J. Zhang and K. Zhang, *Int. J. Plast.*, 115 (2019) 293.
15. Y.H. Suo, F.Q. Yang, *Acta Mech.*, 230 (2019) 993.
16. Y.T. Cheng, M.W. Verbrugge, *J. Power Sources*, 190 (2009) 453.
17. X.C. Zhang, A.M. Sastry and W. Shyy, *J. Electrochem. Soc.*, 155 (2008) A542.
18. H. Zheng, J. Gao, S. F. Wang and H. Li, *Energy Storage Sci. Technol.*, 2 (2013) 620.
19. S. Golmon, K. Maute, S.H. Lee and L.D. Martin, *Appl. Phys. Lett.*, 97 (2010) 033111.
20. T.H. Wan, F. Ciucci, Continuum level transport and electro-chemo-mechanics coupling-solid oxide fuel cells and lithium ion batteries, *Electro-Chemo-Mechanics of Solids*, Cham, Switzerland, 2017, 161-189.
21. H. Dal, C. Miehe, *Comput. Mech.*, 55 (2015) 303.
22. S. Mohanty, P.Y. Kumbhar, R.K. Annabattula and N. Swaminathan, *Solid State Ionics*, 342 (2019) 115053.
23. W.X. Mei, Q.L. Duan, P. Qin, J.J. Xu, Q.S. Wang and J.H. Sun, *J. Electrochem. Soc.*, 166 (2019) A3319.
24. J. Chen, G.W. Ma, *Int. J. Numer. Methods Eng.*, 68 (2006) 1052.
25. J.C.M. Li, *Metall. Mater. Trans. A*, 9 (1978) 1353.

26. W.B. Zhou, *Electrochim. Acta*, 185 (2015) 28.
27. D.M. Zhou, Y.S. Deng, C.F. Ying, Y.C. Zhang, Y.X. Feng, Q.M. Huang, L.Y. Liang and D.Q. Wang, *Chin. Phys. Lett.*, 33 (2016) 108501.
28. M.Q. Guo, X.G. Zhang, Z.C. Bai, J.Y. Ye, W.J. Meng, H. Song and Z.H. Wang, *Int. J. Hydrogen Energy*, 42 (2017) 15290.
29. Y.H. Hu, X.H. Zhao and Z.G. Suo, *J. Mater. Res.*, 25 (2010) 1007.
30. Y.Z. Peng, K. Zhang, B.L. Zheng and Y. Li, *Acta Phys. Sin.*, 65 (2016) 100201. (in Chinese)

© 2020 The Authors. Published by ESG (www.electrochemsci.org). This article is an open access article distributed under the terms and conditions of the Creative Commons Attribution license (<http://creativecommons.org/licenses/by/4.0/>).